ESC HEART FAILURE
ESC Heart Failure (2019)
Published online in Wiley Online Library (wileyonlinelibrary.com) **DOI:** 10.1002/ehf2.12576

ORIGINAL RESEARCH ARTICLE

Comparison of feature tracking, fast-SENC, and myocardial tagging for global and segmental left ventricular strain

Paulius Bucius[1,2], Jennifer Erley[1], Radu Tanacli[1], Victoria Zieschang[1], Sorin Giusca[3], Grigorious Korosoglou[3], Henning Steen[4], Christian Stehning[5], Burkert Pieske[1,6,7], Elisabeth Pieske-Kraigher[6,7], Andreas Schuster[8], Tomas Lapinskas[1,2,6] and Sebastian Kelle[1,6,7]*

[1]*Department of Internal Medicine/Cardiology, German Heart Center Berlin, Berlin, Germany;* [2]*Department of Cardiology, Medical Academy, Lithuanian University of Health Sciences, Kaunas, Lithuania;* [3]*Department of Cardiology and Vascular Medicine, GRN Hospital Weinheim, Weinheim, Germany;* [4]*Department of Internal Medicine/Cardiology, Marienkrankenhaus Hamburg, Hamburg, Germany;* [5]*Philips Healthcare, Hamburg, Germany;* [6]*DZHK (German Centre for Cardiovascular Research), Partner Site Berlin, Berlin, Germany;* [7]*Department of Internal Medicine/Cardiology, Charité Campus Virchow Clinic, Berlin, Germany;* [8]*Department of Cardiology and Pneumology, University Medical Center Göttingen, Georg-August University, Göttingen, Germany*

Abstract

Aims A multitude of cardiac magnetic resonance (CMR) techniques are used for myocardial strain assessment; however, studies comparing them are limited. We sought to compare global longitudinal (GLS), circumferential (GCS), segmental longitudinal (SLS), and segmental circumferential (SCS) strain values, as well as reproducibility between CMR feature tracking (FT), tagging (TAG), and fast-strain-encoded (fast-SENC) CMR techniques.

Methods and results Eighteen subjects (11 healthy volunteers and seven patients with heart failure) underwent two CMR scans (1.5T, Philips) with identical parameters. Global and segmental strain values were measured using FT (Medis), TAG (Medviso), and fast-SENC (Myocardial Solutions). Friedman's test, linear regression, Pearson's correlation coefficient, and Bland–Altman analyses were used to assess differences and correlation in measured GLS and GCS between the techniques. Two-way mixed intra-class correlation coefficient (ICC), coefficient of variance (COV), and Bland–Altman analysis were used for reproducibility assessment.

All techniques correlated closely for GLS (Pearson's *r*: 0.86–0.92) and GCS (Pearson's *r*: 0.85–0.94). Intra-observer and inter-observer reproducibility was excellent in all techniques for both GLS (ICC 0.92–0.99, CoV 2.6–10.1%) and GCS (ICC 0.89–0.99, CoV 4.3–10.1%). Inter-study reproducibility was similar for all techniques for GLS (ICC 0.91–0.96, CoV 9.1–10.8%) and GCS (ICC 0.95–0.97, CoV 7.6–10.4%). Combined segmental intra-observer reproducibility was good in all techniques for SLS (ICC 0.914–0.953, CoV 12.35–24.73%) and SCS (ICC 0.885–0.978, CoV 10.76–19.66%). Combined inter-study SLS reproducibility was the worst in FT (ICC 0.329, CoV 42.99%), while fast-SENC performed the best (ICC 0.844, CoV 21.92%). TAG had the best reproducibility for combined inter-study SCS (ICC 0.902, CoV 19.08%), while FT performed the worst (ICC 0.766, CoV 32.35%). Bland–Altman analysis revealed considerable inter-technique biases for GLS (FT vs. fast-SENC 3.71%; FT vs. TAG 8.35%; and TAG vs. fast-SENC 4.54%) and GCS (FT vs. fast-SENC 2.15%; FT vs. TAG 6.92%; and TAG vs. fast-SENC 2.15%). Limits of agreement for GLS ranged from ±3.1 (TAG vs. fast-SENC) to ±4.85 (FT vs. TAG) for GLS and ±2.98 (TAG vs. fast-SENC) to ±5.85 (FT vs. TAG) for GCS.

Conclusions We found significant differences in measured GLS and GCS between FT, TAG, and fast-SENC. Global strain reproducibility was excellent for all techniques. Acquisition-based techniques had better reproducibility than FT for segmental strain.

Keywords Myocardial deformation; Strain; Cardiac magnetic resonance; SENC; Tagging; Feature tracking

Received: 3 July 2019; Revised: 10 October 2019; Accepted: 11 November 2019
**Correspondence to: Professor Sebastian Kelle, MD (FSCMR, FESC, FAHA), Department of Internal Medicine/Cardiology, German Heart Center Berlin and Charité University Medicine Berlin, Augustenburger Platz 1, 13353 Berlin, Germany. Tel: +49-30-4593 1182; Fax: +49-30-4593 2500. Email: kelle@dhzb.de*

Introduction

Myocardial strain imaging has been shown to be useful in identification and risk stratification of a wide range of cardiac conditions.[1,2] In certain conditions, its decline precedes that of the left ventricular ejection fraction (LVEF),[3,4] which shows promise for it to become a supplementary tool for early diagnostics.

Since the inception of myocardial strain imaging in a form of cardiac magnetic resonance (CMR) myocardial tagging (TAG) in 1988 by Zerhouni et al.,[5] it has rapidly spread inside the field of CMR. From 1990s to early 2000s, multiple acquisition-based CMR methods emerged as means to calculate myocardial deformation parameters. TAG has been extensively studied, validated, and shown to be a highly reproducible method for measurement of myocardial deformation.[6] Despite its advantages, the usability of TAG is hampered by long acquisition and post-processing times.[7] More recently, displacement encoding with stimulated echoes,[8] strain-encoded CMR imaging (SENC),[9] and fast-strain-encoded CMR imaging (fast-SENC)[10] emerged as alternatives to TAG, offering faster acquisition and post-processing, as well as excellent reproducibility.[11,12] Despite these advantages, all these techniques require acquisition of additional imaging sequences. In contrast, CMR feature tracking (FT) is a post-processing-based method that allows quantification of strain parameters from standard steady-state free precession (SSFP) cine images, clinically used for functional analysis of the heart. Given the fact that FT does not require additional imaging sequences and has a short post-processing time, it is now considered a preferred technique for myocardial deformation assessment.[7] Each modality has its own advantages and disadvantages; however, given the acquisition and post-processing differences, variation in measured strain parameters is inevitable.

With this study, we sought to explore the differences in global left ventricular (LV) strain measurements derived using FT, fast-SENC, and TAG in a population of healthy subjects and heart failure (HF) patients. We also assessed the reproducibility and variability of the aforementioned modalities at intra-observer, inter-observer, and inter-study levels for global strain and intra-observer and inter-study levels for segmental strain.

Methods

Study population

In a period between March 2017 and September 2017, 11 healthy volunteers and seven HF patients [four with preserved LVEF (three of which with diastolic dysfuncion and one with aortic stenosis) and three with reduced LVEF of ischaemic origin] were included in the study; two CMR scans were performed on each participant, using an identical imaging protocol. Approval for the study was acquired from the Ethics Committee of Charité–Universitäts Medizin Berlin. The study complied with the declaration of Helsinki. Informed consent was given by all participants of the study.

Cardiovascular magnetic resonance acquisition

Cardiovascular magnetic resonance scans were performed on a 1.5 Tesla MRI scanner (Achieva, Philips Healthcare, Best, the Netherlands). A five-element-phased array cardiac coil was used for signal reception. Four-lead vector electrocardiogram was used for R-wave triggering. Images for FT, fast-SENC, and TAG were acquired in long-axis (LAX) 2-chamber, 3-chamber, and 4-chamber views, as well as a short-axis (SAX) stack. Balanced SSFP sequence with breath hold was used for FT analysis with the following acquisition parameters: repetition time (TR) = 3.3 ms, echo time (TE) = 1.6 ms, flip angle = 60°, acquisition voxel size = 1.8 × 1.7 × 8.0 mm^3, and 30 phases per cardiac cycle. A single-breath hold, cardiac-triggered 2D TAG sequence was employed using an orthogonal saturation grid, with a grid spacing of 7 mm and a tag grid angle of 45°. Typical parameters of the subsequent imaging protocol were as follows: field of view = 340 × 340 mm^2, slice thickness = 8 mm, voxel size = 1.9 × 1.9 × 8 mm^3, reconstructed solution at 1.2 × 1.2 × 8 mm^3, flip angle = 15°, TE = 1.8 ms, TR = 4.2 ms, temporal resolution = 55 ms, typical number of acquired heart phases = 16, and acquisition time per slice = 18 s. No parallel imaging was employed. A recently developed real-time free-breathing fast-SENC imaging technique (Myocardial Solutions, Inc., Morrisville, North Carolina, USA)[10] was used for fast-SENC strain assessment. The following acquisition parameters were used: field of view = 256 × 256 mm^2, slice thickness 10 mm, voxel size 4 × 4 × 10 mm^3, reconstructed resolution at 1 × 1 × 10 mm^3 using zero-filled interpolation (in-plane ZIP 1024), single-shot spiral readout (three interleaves) with acquisition time = 10 ms, flip angle = 30°, TE = 0.7 ms, TR = 12 ms, temporal resolution = 36 ms, typical number of acquired heart phases = 22, spectrally selective fat suppression, and total acquisition time per slice <1 s.

Feature tracking analysis

Feature tracking analysis was performed offline using commercially available software (Medis Suite, version 3.1, Leiden, the Netherlands). Endocardial borders of the left ventricle were outlined in end-diastolic frame of the three LAX and three SAX (basal, mid-ventricular, and apical) images. Following an automatic propagation, adjustments were made to the contours where needed. Endocardial global longitudinal

strain (GLS) and circumferential strain (GCS) were derived by averaging the peak strain values of individual segments using 17 and 16 segment models.

Tagging analysis

Tagging-derived strain parameters were acquired using a commercially available software Segment version 2.2 R6960 (http://segment.heiberg.se).[13] Endocardial and epicardial borders were outlined in end-systolic time frame of three LAX and SAX (basal, mid-ventricular, and apical) images. Automatic propagation algorithm was then applied, and necessary corrections were made by the observer. GLS and GCS parameters were derived by averaging the peak strain values of individual segments using 17 and 16 segments models.

Fast-strain-encoded cardiovascular magnetic resonance imaging analysis

Fast-SENC images were uploaded from the scanner into dedicated, commercially available MyoStrain software (Myocardial Solutions, Inc.). Endocardial and epicardial borders were outlined in three LAX and three SAX images at an end-systolic time frame. Necessary manual adjustments were made after automatic propagation by the software to ensure sufficient tracking throughout the cardiac cycle. LS values were extracted from the SAX images using a 16 segment model. Circumferential strain values were acquired from LAX images: GCS was calculated by averaging the peak strain values from a 17 segment model, while seven segments per slice (21 total segments), as provided by the software, were used for segmental comparison.

Given the counterintuitive nature of negative strain values becoming more positive in diseased subjects, absolute values of GCS and GLS are reported for easier interpretation of the results.

Intra-observer and inter-observer reproducibility

Every scan was analysed by two experienced raters in each modality for inter-observer variability testing. In order to determine the intra-observer variability, 10 randomly selected cases were analysed a second time by one of the observers after a minimum period of 4 weeks to ensure there was no recall bias. All observers were blinded to prior investigations and clinical data of the subjects.

Inter-study reproducibility

A second CMR scan with identical imaging parameters was performed in all of the individuals. Median time between the two scans was 40 days. There was no change in medication or symptoms of the HF patients in between the scans. Additionally, we excluded new onset of cardiac disease in the healthy subjects. In order to prevent recall bias, the second scan was analysed after a minimum of 4 weeks by one of the observers, who was blinded to the results of the first scan and clinical data of the subjects.

Segmental comparison

Intra-observer and inter-study comparison was also performed on segmental basis for both segmental longitudinal (SLS) and segmental circumferential strain (SCS). Each technique was assessed by comparing the results of the first and the second measurement in individual segments first and then by pooling the data of all the segments to get a combined value.

Statistical analysis

Commercially available statistical analysis software (GraphPad Prism 8, GraphPad Software, San Diego, CA, USA) was used for statistical analysis. Continuous variables are expressed as either mean ± standard deviation or median ± interquartile range, according to normality of distribution, assessed by Shapiro–Wilk test. Strain measurements from three modalities were compared using Friedman's test with Dunn's post hoc test for pair-wise comparison. Linear regression analysis was used to assess the correlation between the imaging modalities, followed by Bland–Altman analysis of the mean bias and limits of agreement (LOA). Inter-observer and intra-observer, as well as inter-study variability, were assessed using the intra-class correlation coefficient (ICC) for absolute agreement and coefficient of variance (CoV), defined as standard deviation of the differences divided by the mean.[14] Agreement levels were defined according to previous studies[15]: excellent for ICC $>$ 0.74, good for ICC 0.6–0.74, fair for ICC 0.4–0.59, and poor for ICC $<$0.4. Segmental intra-observer and inter-study variability and agreement was assessed using ICC and CoV. Alpha level of 0.05 and below was considered statistically significant.

Results

Global longitudinal strain

Global longitudinal strain measured by FT showed a trend towards being higher than that measured by fast-SENC (*P* value = 0.05), while fast-SENC-derived GLS was significantly higher than TAG (*Figure 1* and *Table 1*). Excellent correlation was observed between the three modalities.

Figure 1 Comparison of GLS (A) and GCS (B) measured using three CMR modalities. Results of Friedman's test with Dunn's post hoc analysis: ns—$P \geq 0.05$, *—$P < 0.05$, ***—$P < 0.001$. FT, feature tracking; GCS, global circumferential strain; GLS, global longitudinal strain; SENC, strain-encoded magnetic resonance imaging; TAG, myocardial tagging.

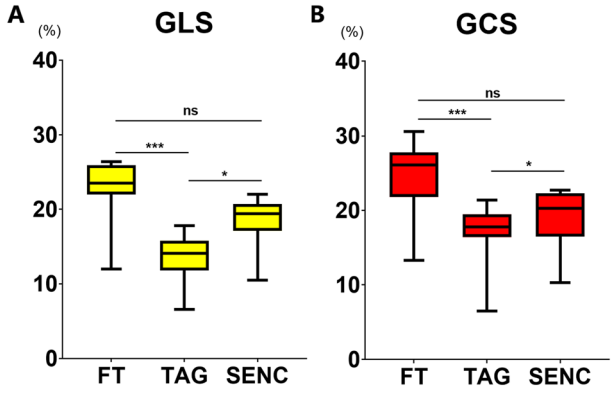

Table 1 Global strain values derived from different cardiovascular magnetic resonance techniques

	FT	TAG	SENC
GLS (%)	23.5 (22.0–25.9)	14.9 (11.8–16.9)	19.4 (17.1–20.7)
GCS (%)	26.1 (21.8–27.8)	17.8 (16.4–19.5)	20.3 (16.5–22.3)

Values are expressed as median (interquartile range). FT, feature tracking; GCS, global circumferential strain; GLS, global longitudinal strain; SENC, fast-strain-encoded cardiovascular magnetic resonance; TAG, myocardial tagging.

FT and fast-SENC had the closest correlation ($r = 0.924$, $P < 0.001$). Linear regression analyses and Bland–Altman comparisons for GLS are depicted in *Figure 2*. Visual representation of differences in measured GLS between the techniques is depicted in *Figure 3*.

Global circumferential strain

Global circumferential strain measured by FT showed a trend towards being greater than fast-SENC ($P = 0.05$), while TAG-derived GCS was significantly lower than fast-SENC (*Figure 1* and *Table 1*). All three modalities correlated closely with each other. TAG and fast-SENC had the closest correlation ($r = 0.938$, $P < 0.001$) and narrowest LOA (±3.1), as depicted in *Figure 4*. Visual representation of differences in measured GLS between the techniques is depicted in *Figure 5*.

Feasibility

Feature tracking and fast-SENC analysis were successful in every scan, giving a feasibility of 100%. TAG analysis was not possible in 5/36 scans due to breathing artefacts, thus it was the method with the worst feasibility −86.1%. Direct comparison between all modalities was possible in 31 cases, and 36 cases were used for FT and fast-SENC comparison.

Intra-observer and inter-observer reproducibility

Intra-observer and inter-observer variability results are depicted in *Table 2*. Fast-SENC showed the least variability and highest reproducibility, followed by TAG and FT, respectively.

Figure 2 Linear regression and Bland–Altman analyses for global longitudinal strain comparison between FT vs. TAG, FT vs. FAST-SENC, and FAST-SENC vs. TAG. FT, feature tracking; SENC, strain-encoded magnetic resonance imaging; TAG, myocardial tagging.

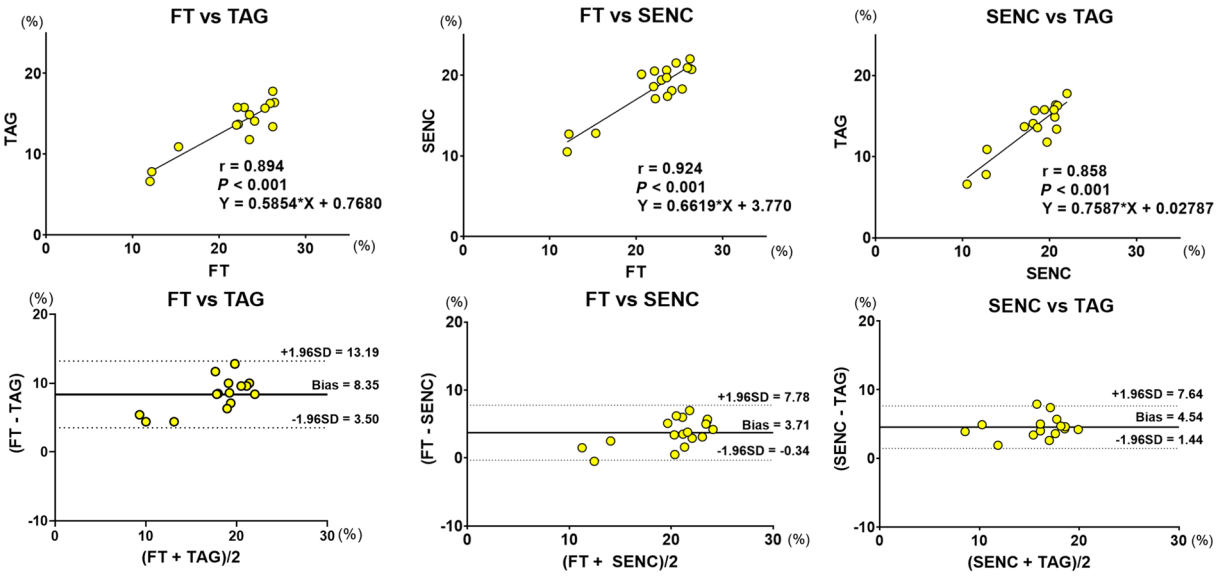

DOI: 10.1002/ehf2.12576

Figure 3 Visual representation of GLS assessment with the three different cardiovascular magnetic resonance techniques. TAG on the left, SENC on the right, and FT on the top picture. Mean difference (bias) between techniques, derived from Bland–Altman analyses, is shown. FT, feature tracking; GLS, global longitudinal strain; SENC, strain-encoded magnetic resonance imaging; TAG, myocardial tagging.

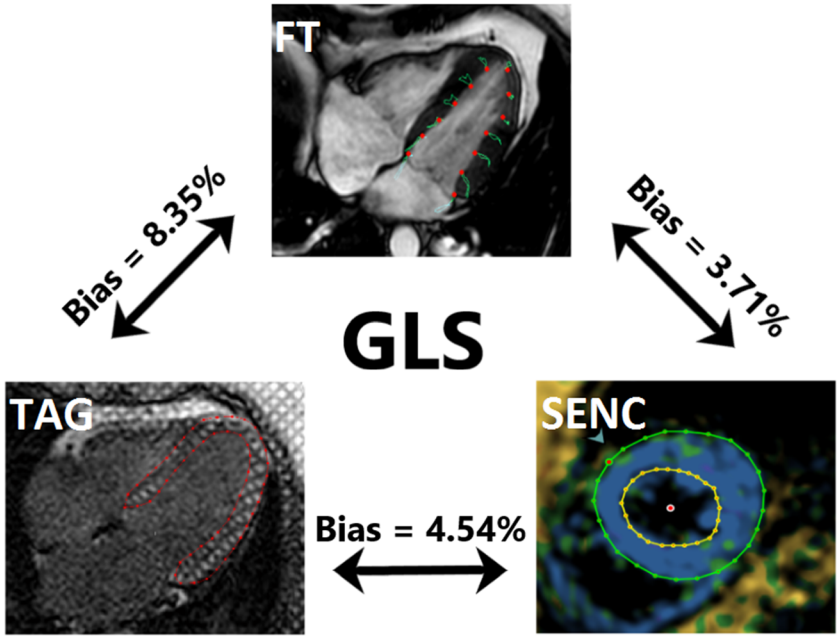

Inter-study reproducibility

We found excellent inter-study reproducibility in all of the techniques, as shown by measured ICCs (GLS: for FT = 0.91, $P < 0.001$; for TAG = 0.96, $P < 0.001$; and for fast-SENC = 0.94, $P < 0.001$; GCS: for FT = 0.97, $P < 0.001$; for TAG = 0.95, $P < 0.001$; and for fast-SENC = 0.96, $P < 0.001$). LOA, CoV, and inter-study biases are depicted in *Table 2*.

Segmental reproducibility

Values of combined segmental strain reproducibility comparison are depicted in *Table 3*, and values for individual

Figure 4 Linear regression and Bland–Altman analyses for global circumferential strain comparison between FT vs. TAG, FT vs. fast-SENC, and fast-SENC vs. TAG. FT, feature tracking; SENC, strain-encoded magnetic resonance imaging; TAG, myocardial tagging.

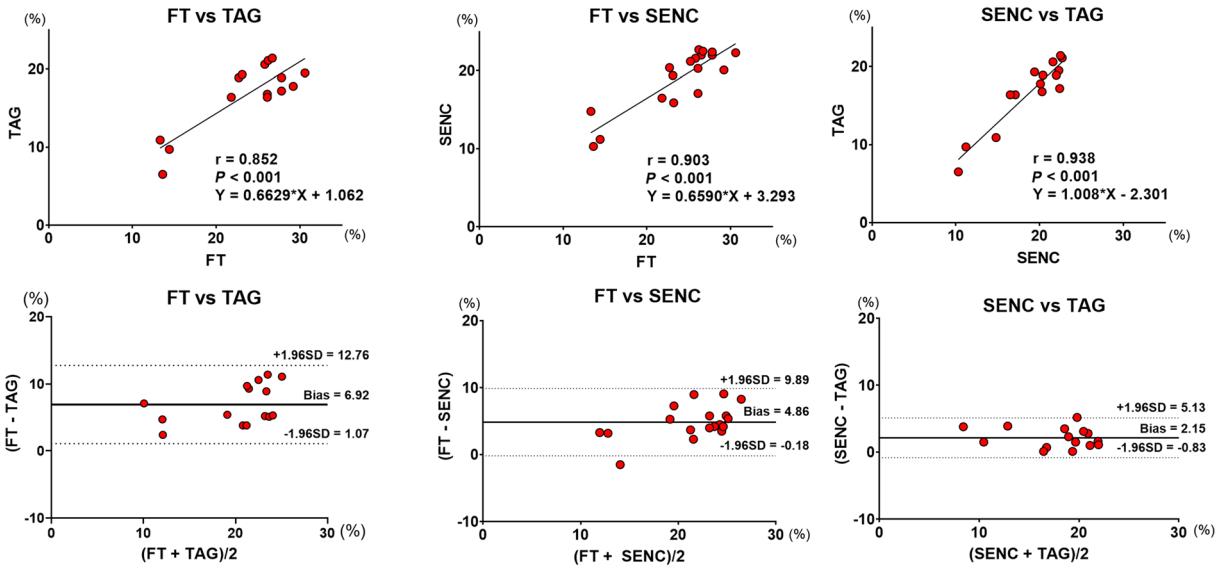

DOI: 10.1002/ehf2.12576

Figure 5 Visual representation of global longitudinal strain assessment with the three different cardiovascular magnetic resonance techniques. TAG on the left, SENC on the right, and FT on the top picture. Mean difference (bias) between techniques, derived from Bland–Altman analyses, is shown. FT, feature tracking; GCS, global circumferential strain; SENC, strain-encoded magnetic resonance imaging; TAG, myocardial tagging.

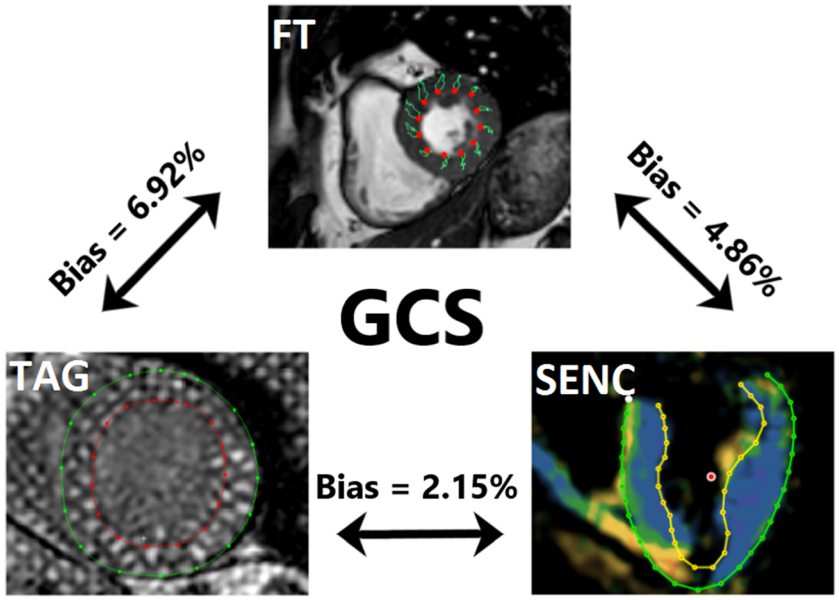

Table 2 Comparison of reproducibility of global strain parameters

	Bias (%)	Limits of agreement (±)	CoV (%)	ICC
		Intra-observer reproducibility		
FT				
GLS	−0.32	1.6	3.8	0.95
GCS	0.94	3.45	6.2	0.89
TAG				
GLS	0.07	1.7	6.7	0.99
GCS	−0.2	1.6	5	0.99
SENC				
GLS	−0.03	0.6	1.5	0.99
GCS	0.14	1.15	3.11	0.99
		Inter-observer reproducibility		
FT				
GLS	0.6	6.2	10.1	0.92
GCS	−3.3	5.0	10.1	0.86
TAG				
GLS	0.04	2.0	7.7	0.98
GCS	−0.5	2.7	8.2	0.97
SENC				
GLS	0.1	1.0	2.6	0.99
GCS	0.3	1.6	4.3	0.99
		Inter-study reproducibility		
FT				
GLS	−0.69	4.7	10.8	0.91
GCS	0.37	3.5	7.6	0.97
TAG				
GLS	−0.42	2.5	9.4	0.96
GCS	−0.78	3.5	10.4	0.95
SENC				
GLS	−0.15	3.3	9.1	0.94
GCS	−0.27	3.3	8.9	0.96

CoV, coefficient of variance; FT, feature tracking; GCS, global circumferential strain; GLS, global longitudinal strain; ICC, intra-class correlation coefficient; SENC, fast-strain-encoded cardiovascular magnetic resonance imaging; TAG, myocardial tagging.

segments are presented in Supporting Information, *Tables* S1–S6. Combined intra-observer agreement was excellent in all of the techniques in both SLS (ICC: for FT = 0.914, $P < 0.001$; for TAG = 0.915, $P < 0.001$; and for fast-SENC = 0.953, $P < 0.001$) and SCS (ICC: for FT = 0.885, $P < 0.001$; for TAG = 0.978, $P < 0.001$; and for fast-SENC = 0.932, $P < 0.001$). SLS derived from fast-SENC had the lowest variation (CoV = 12.35%), followed by FT (CoV = 21.87%) and TAG (CoV = 24.73%). TAG showed the lowest variability for SCS (CoV = 10.76%), followed by fast-SENC (CoV = 17.59%) and FT (CoV = 19.66%). Inter-study agreement for SLS was poor for FT (ICC = 0.329, $P < 0.001$), while TAG and fast-SENC showed excellent agreement (ICC = 0.768, $P < 0.001$ and 0.844, $P < 0.001$, respectively). All of the modalities showed excellent inter-study agreement for SCS (ICC: for FT = 0.766, $P < 0.001$; for TAG = 0.902, $P < 0.001$; and for fast-SENC = 0.850, $P < 0.001$). Fast-SENC had the lowest variation for SLS (CoV = 21.92%), followed by TAG (CoV = 37.75%) and FT (CoV = 42.99%). As in intra-observer comparison, TAG performed the best for SCS (CoV = 19.08%), followed by fast-SENC (CoV = 23.52%) and FT (CoV = 32.35%).

Discussion

Speckle tracking echocardiography-derived strain values are recommended for clinical use by both European Society of Cardiology and American Heart Assosiation,[16] thus highlighting the current and future importance of strain imaging.

Table 3 Comparison of reproducibility of combined segmental strain parameters

		FT		TAG		SENC	
		Intra-observer	Inter-study	Intra-observer	Inter-study	Intra-observer	Inter-study
ICC	SLS	0.914	0.329	0.915	0.768	0.953	0.844
	SCS	0.885	0.766	0.978	0.902	0.932	0.850
COV (%)	SLS	21.87	42.99	24.73	37.75	12.35	21.92
	SCS	19.66	32.35	10.76	19.08	17.59	23.52

CoV, coefficient of variance; FT, feature tracking; ICC, intra-class correlation coefficient; SCS, segmental circumferential strain; SENC, fast-strain-encoded cardiovascular magnetic resonance imaging; SLS, segmental longitudinal strain; TAG, myocardial tagging.

Given the fact that CMR can overcome most of the echocardiography's inborn shortcomings, we expect CMR to become a more reliable tool for future deformation imaging. Indeed, CMR-derived strain has been shown to be more reproducible and to have better feasibility.[17] However, despite CMRs advantages over echocardiography and promising studies regarding its possible usefulness in the clinical setting, the multitude of techniques for strain assessment, as well as inter-vendor differences within these techniques,[18,19] hinder further clinical applicability of these measurements. In order for CMR-based strain measurements to become clinically useful, a standardization of available techniques is necessary.

The design of our study allowed for a direct comparison and exploration of differences between three widely used CMR-based strain measurement techniques. The main findings of our study are as follows:

(1) There was significant bias between the three imaging techniques in measured GLS and GCS.
(2) There was excellent correlation for both GLS and GCS between the three modalities tested.
(3) Agreement and variability for intra-observer and inter-observer, as well as inter-study global strain measurements, was excellent in all three modalities.
(4) Segmental strain comparison showed excellent intra-observer agreement in all three modalities. TAG and fast-SENC had better inter-study agreement than FT for segmental strain.

TAG has been historically considered the gold standard technique for strain assessment. It has been shown to be highly reproducible and used for validation of other strain assessment techniques.[20,21] However, it requires long acquisition and post-processing times, in addition to suffering from low temporal and spatial resolutions, as well as tag fading during the diastole. Furthermore, in our cohort, TAG images could not be assessed in approximately 1/7th of all scans due to artefacts. In comparison, fast-SENC, despite also requiring acquisition of additional sequences, is a one heartbeat, free-breathing technique with quick post-processing.[22] Our intra-observer and inter-observer comparisons show it to be more robust than TAG and to have comparable inter-study reproducibility. Furthermore, a recent study by Lapinskas et al.[23] demonstrated feasibility of fast-SENC to assess LV volumes and LVEF, making it a convenient option for functional assessment of the heart. Such short acquisition and post-processing times make fast-SENC technique very attractive in daily routine, especially in severely ill patients and children.[22] It must be noted that due to technical limitations, radial strain cannot be assessed from SENC acquisitions.[7] Additionally, it has a worse spatial resolution than TAG and FT.[22] On the other end of the spectrum, FT is a post-processing technique that does not require additional image acquisition. This gives FT an advantage for use in a clinical setting, as it can retrospectively be applied to SSFP images, acquired using a clinically standard CMR protocol. Furthermore, in our comparison, FT had excellent reproducibility and correlation with both TAG and fast-SENC. To sum up, both fast-SENC and FT possess certain advantages over the gold standard that make them more attractive for clinical use, while still maintaining robustness.

Although not apparent in global comparison, variability in segmental comparison was consistently higher in strain derived from LAX images, as compared with SAX images. It is in-line with previously published studies[24] and can be explained by poor tracking of basal segments in LAX images due to complex architecture of the mitral annulus.[7] It would also explain why fast-SENC had by far the lowest variability in SLS comparison, although it was outperformed by TAG for SCS. Furthermore, fast-SENC was also the most robust modality in GLS comparisons. Given the fact that GLS is the most widely validated and the only clinically used strain measurement, fast-SENC could be a method of choice for future studies. Of note, FT performed worse than both acquisition-based techniques in segmental comparisons. It also had poor inter-study variability for both SCS (CoV 32.35%) and SLS (CoV 42.99%), supporting the opinions of previous authors that FT is not ready for use in segmental strain assessment.[25,26] This may have significant implications especially in the detection of regional LV dysfunction, for example, in patients with suspected or known ischaemic heart disease. Additionally, by comparing intra-observer reproducibility of GCS between observers with different levels of experience, Feisst et al. demonstrated that reproducibility of FT is highly dependent on observer experience.[27] Since reproducibility

of the global measurements in our study closely matches that of an experienced observer from the aforementioned study, the results of our segmental comparison are indicative of a best-case scenario. Furthermore, a recent study by Backhaus et al. assessed the impact of observer training on reproducibility of FT strain measurements from three different vendors and found that the positive impact of observer experience is present independently of vendor choice.[28]

It must also be highlighted that, despite excellent correlation and reproducibility of these techniques for global measurements, significant differences in measured strain between the modalities were detected in our study. The fact that our study design accounted for possible subject-related biases, such as different loading conditions, points towards a systematic difference between the techniques in question. Indeed, a recent meta-analysis by Vo et al.[29] sought to find normal values for CMR-derived strain parameters and reported similar albeit less pronounced differences in GLS and GCS between these modalities. The observed differences can at least in part be explained by looking at how the strain values are derived in each technique. FT is a post-processing method that uses SSFP images to identify certain features within these images and tries to track them throughout the successive frames of the cine loop. However, through-plane movement can cause some of the tracked features to move out of the imaging plane and be replaced by other regions of the myocardium, thus causing through-plane motion artefacts. Furthermore, for FT, we reported endocardial strain values, which are naturally higher.[2] On the other hand, both TAG and fast-SENC are acquisition-based techniques and, as such, are not affected by through-plane motion artefacts. However, the latter uses parallel tags as opposed to orthogonal ones used in the former. Therefore, SAX images are used to acquire longitudinal strain, while circumferential strain is derived from the LAX images, essentially meaning that these techniques acquire strain measurements at different spatial points. In the end, even though all of these techniques employ CMR for image acquisition, there are fundamental differences in imaging protocols and analysis algorithms that ultimately amount to substantial bias.

Our study supports the previously expressed opinion that before further standardization is brought forward, different CMR modalities cannot be used interchangeably for strain assessment.[18] However, reproducibility analysis of global measurements showed excellent results for all three techniques, which is encouraging for a shift towards clinical use, as excellent inter-study reproducibility is paramount in follow-up scans for assessment of disease progression.

Limitations

The main limitation of this study was a relatively small sample size. However, our cohort included both healthy volunteers and HF patients with reduced and preserved LVEF. Secondly, images were analysed using different software solutions dedicated for each modality, thus inter-vendor differences could not be explored. Nonetheless, all the software solutions used in our study are validated and commercially available.

Conclusions

Important differences in measured GLS and GCS exist between FT, TAG, and fast-SENC, thus care should be taken when comparing these values. There was excellent GLS and GCS reproducibility at intra-observer, inter-observer, and inter-study levels and close correlation between these modalities. Acquisition-based techniques had better reproducibility than FT for segmental strain. Fast-SENC had the lowest variability for SLS, while TAG performed the best for SCS.

Conflict of interest

Authors declare no competing interests.

Author contributions

P.B. performed image and statistical analysis and drafted the manuscript. J.E., R.T., V.Z., S.G., and T.L. performed image analysis. J.E., S.G., G.K., H.S., B.P., E.P.K., A.S., T.L., and S.K. provided critical revision of the manuscript. G.K., H.S., B.P., E.P.K., A.S., and S.K. designed the study. C.S. acquired images and helped with drafting the manuscript. S.K. provided the conception of the study.

Funding

S.K. received an unrestricted research grant by Philips Healthcare and a research grant from Myocardial Solutions. S.K., T.L., B.P., A.S., and E.P.K. are supported by the DZHK (German Centre for Cardiovascular Research) and by the BMBF (German Ministry of Education and Research).

Availability of data and material

The datasets used and/or analysed during the current study are available from the corresponding author on reasonable request.

Supporting information

Additional supporting information may be found online in the Supporting Information section at the end of the article.

Table S1. Segmental comparison of ICC for FT.
Table S2. Segmental comparison of ICC for TAG.
Table S3. Segmental comparison of ICC for SENC.
Table S4. Segmental comparison of CoV for FT.
Table S5. Segmental comparison of CoV for TAG.
Table S6. Segmental comparison of CoV for SENC.
Table S7. Haemodynamic status of study subjects during the first and second MRI scan.

References

1. Choi E-Y, Rosen BD, Fernandes VRS, Yan RT, Yoneyama K, Donekal S, Opdahl A, Almeida ALC, Wu CO, Gomes AS, Bluemke DA, Lima JAC. Prognostic value of myocardial circumferential strain for incident heart failure and cardiovascular events in asymptomatic individuals: the Multi-Ethnic Study of Atherosclerosis. *Eur Heart J [Internet]*. 2013 Aug 7; **34**: 2354–2361.
2. Smiseth OA, Torp H, Opdahl A, Haugaa KH, Urheim S. Myocardial strain imaging: how useful is it in clinical decision making? *Eur Heart J [Internet]*. 2016 Apr 14; **37**: 1196–1207.
3. Negishi K, Negishi T, Haluska BA, Hare JL, Plana JC, Marwick TH. Use of speckle strain to assess left ventricular responses to cardiotoxic chemotherapy and cardioprotection. *Eur Hear J - Cardiovasc Imaging [Internet]*. 2014 Mar 1; **15**: 324–331.
4. Urbano-Moral JA, Rowin EJ, Maron MS, Crean A, Pandian NG. Investigation of global and regional myocardial mechanics with 3-dimensional speckle tracking echocardiography and relations to hypertrophy and fibrosis in hypertrophic cardiomyopathy. *Circ Cardiovasc Imaging [Internet]*. 2014 Jan; **7**: 11–19.
5. Zerhouni EA, Parish DM, Rogers WJ, Yang A, Shapiro EP. Human heart: tagging with MR imaging—a method for noninvasive assessment of myocardial motion. *Radiology [Internet]*. 1988 Oct; **169**: 59–63.
6. Swoboda PP, Larghat A, Zaman A, Fairbairn TA, Motwani M, Greenwood JP, Plein S. Reproducibility of myocardial strain and left ventricular twist measured using complementary spatial modulation of magnetization. *J Magn Reson Imaging [Internet]*. 2014 Apr; **39**: 887–894.
7. Scatteia A, Baritussio A, Bucciarelli-Ducci C. Strain imaging using cardiac magnetic resonance. *Heart Fail Rev [Internet]*. 2017 Jul 15; **22**: 465–476.
8. Feng L, Donnino R, Babb J, Axel L, Kim D. Numerical and in vivo validation of fast cine displacement-encoded with stimulated echoes (DENSE) MRI for quantification of regional cardiac function. *Magn Reson Med [Internet]* 2009 Sep; **62**: 682–690. Available from. http://www.ncbi.nlm.nih.gov/pubmed/19585609.
9. Osman NF, Sampath S, Atalar E, Prince JL. Imaging longitudinal cardiac strain on short-axis images using strain-encoded MRI. *Magn Reson Med [Internet]*. 2001 Aug; **46**: 324–334.
10. Pan L, Stuber M, Kraitchman DL, Fritzges DL, Gilson WD, Osman NF. Real-time imaging of regional myocardial function using fast-SENC. *Magn Reson Med [Internet]* 2006 Feb; **55**: 386–395. Available from. http://www.ncbi.nlm.nih.gov/pubmed/16402379.
11. Lin K, Meng L, Collins JD, Chowdhary V, Markl M, Carr JC. Reproducibility of cine displacement encoding with stimulated echoes (DENSE) in human subjects. *Magn Reson Imaging [Internet]* 2017 Jan; **35**: 148–153. Available from:. https://linkinghub.elsevier.com/retrieve/pii/S0730725X1630114X.
12. Giusca S, Korosoglou G, Zieschang V, Stoiber L, Schnackenburg B, Stehning C, Gebker R, Pieske B, Schuster A, Backhaus S, Pieske-Kraigher E, Patel A, Kawaji K, Steen H, Lapinskas T, Kelle S. Reproducibility study on myocardial strain assessment using fast-SENC cardiac magnetic resonance imaging. *Sci Rep [Internet]* 2018 Dec; **20**: 14100. Available from:. http://www.nature.com/articles/s41598-018-32226-3.
13. Eds NS, Hutchison D. Functional imaging and modeling of the heart. *Proc 8th Int Conf FIMH 2015 [Internet]* 2015; **9126**: 69121–69121.
14. Cicchetti DV. Guidelines, criteria, and rules of thumb for evaluating normed and standardized assessment instruments in psychology. *Psychol Assess [Internet]* 1994; **6**, **4**: 284–290.
15. Oppo K, Leen E, Angerson WJ, Cooke TG, McArdle CS. Doppler perfusion index: an interobserver and intraobserver reproducibility study. *Radiology [Internet]*. 1998 Aug; **208**: 453–457.
16. Voigt J-U, Pedrizzetti G, Lysyansky P, Marwick TH, Houle H, Baumann R, Pedri S, Ito Y, Abe Y, Metz S, Song JH, Hamilton J, Sengupta PP, Kolias TJ, D'Hooge J, Aurigemma GP, Thomas JD, Badano LP. Definitions for a common standard for 2D speckle tracking echocardiography: consensus document of the EACVI/ASE/Industry Task Force to standardize deformation imaging. *Eur Hear J - Cardiovasc Imaging [Internet]*. 2015 Jan 1;**16**():1–11.
17. Obokata M, Nagata Y, Wu VC-C, Kado Y, Kurabayashi M, Otsuji Y, Takeuchi M. Direct comparison of cardiac magnetic resonance feature tracking and 2D/3D echocardiography speckle tracking for evaluation of global left ventricular strain. *Eur Hear J – Cardiovasc Imaging [Internet]*. 2016 May; **17**: 525–532.
18. Cao JJ, Ngai N, Duncanson L, Cheng J, Gliganic K, Chen Q. A comparison of both DENSE and feature tracking techniques with tagging for the cardiovascular magnetic resonance assessment of myocardial strain. *J Cardiovasc Magn Reson [Internet]*. 2018 Dec 19;**20**():26.
19. Beerbaum P, Lotz J, Bigalke B, Fasshauer M, Kowallick JT, Steinmetz M, Hasenfuß G, Staab W, Lamata P, Ritter C, Sohns JM, Unterberg-Buchwald C, Stahnke V-C, Kutty S, Schuster A. Cardiovascular magnetic resonance feature-tracking assessment of myocardial mechanics: intervendor agreement and considerations regarding reproducibility. *Clin Radiol [Internet]*. 2015; **70**: 989–998.
20. Aurich M, Keller M, Greiner S, Steen H, aus dem Siepen F, Riffel J, Katus HA, Buss SJ, Mereles D. Left ventricular mechanics assessed by two-dimensional echocardiography and cardiac magnetic resonance imaging: comparison of high-resolution speckle tracking and feature tracking. *Eur Hear J – Cardiovasc Imaging [Internet]* 2016 Dec; **17**: 1370–1378.
21. Hor KN, Gottliebson WM, Carson C, Wash E, Cnota J, Fleck R, Wansapura J, Klimeczek P, Al-Khalidi HR, Chung ES, Benson DW, Mazur W. Comparison of magnetic resonance feature tracking for strain calculation with harmonic phase imaging analysis. *JACC Cardiovasc Imaging [Internet]*. 2010; **3**: 144–151.
22. Korosoglou G, Giusca S, Hofmann NP, Patel AR, Lapinskas T, Pieske B, Steen H, Katus HA, Kelle S. Strain-encoded magnetic resonance: a method for the assessment of myocardial deformation. *ESC Hear Fail [Internet]* 2019 Apr 25: ehf2.12442.
23. Lapinskas T, Zieschang V, Erley J, Stoiber L, Schnackenburg B, Stehning

C, Gebker R, Patel AR, Kawaji K, Steen H, Zaliunas R, Backhaus SJ, Schuster A, Makowski M, Giusca S, Korosoglou G, Pieske B, Kelle S. Strain-encoded cardiac magnetic resonance imaging: a new approach for fast estimation of left ventricular function. *BMC Cardiovasc Disord [Internet]*. 2019 Mar 5;**19**():52. Available from: http://www.ncbi.nlm.nih.gov/pubmed/30836942

24. Claus P, Omar AMS, Pedrizzetti G, Sengupta PP, Nagel E. Tissue tracking technology for assessing cardiac mechanics. *JACC Cardiovasc Imaging [Internet]*. 2015 Dec; **8**: 1444–1460. Available from:. https://linkinghub.elsevier.com/retrieve/pii/S1936878X15008451.
25. Wu L, Germans T, Güçlü A, Heymans MW, Allaart CP, van Rossum AC. Feature tracking compared with tissue tagging measurements of segmental strain by cardiovascular magnetic resonance. *J Cardiovasc Magn Reson [Internet]*. 2014 Dec 22;**16**():10.
26. Morton G, Schuster A, Jogiya R, Kutty S, Beerbaum P, Nagel E. Inter-study reproducibility of cardiovascular magnetic resonance myocardial feature tracking. *J Cardiovasc Magn Reson [Internet]* 2012; **14**: 43.
27. Feisst A, Kuetting DLR, Dabir D, Luetkens J, Homsi R, Schild HH, Thomas D. Influence of observer experience on cardiac magnetic resonance strain measurements using feature tracking and conventional tagging. *IJC Hear Vasc [Internet]*. 2018 Mar; **18**: 46–51. Available from:. https://linkinghub.elsevier.com/retrieve/pii/S2352906718300332.
28. Backhaus SJ, Metschies G, Billing M, Kowallick JT, Gertz RJ, Lapinskas T, Pieske B, Lotz J, Bigalke B, Kutty S, Hasenfuß G, Beerbaum P, Kelle S, Schuster A. Cardiovascular magnetic resonance imaging feature tracking: impact of training on observer performance and reproducibility. Coelho-Filho OR, editor. *PLoS One [Internet]*. 2019 Jan 25;**14**():e0210127.
29. Vo HQ, Marwick TH, Negishi K. MRI-derived myocardial strain measures in normal subjects. *JACC Cardiovasc Imaging [Internet]*. 2018 Feb; **11**: 196–205. Available from:. https://linkinghub.elsevier.com/retrieve/pii/S1936878X1730253X.